

# A Monte Carlo study of temperature-programmed desorption from supported-metal catalysts

A.S. McLeod and L.F. Gladden

Department of Chemical Engineering, University of Cambridge, Cambridge CB2 3RA, UK  
E-mail: {asm22, gladden}@cheng.cam.ac.uk

Received 19 May 1998; accepted 6 August 1998

The extent to which metal particle geometry and adsorbate spillover influence the temperature-programmed desorption spectra for the desorption of hydrogen from supported-metal catalysts has been studied by Monte Carlo simulation. By including a mechanism for adsorbate spillover and surface diffusion it is shown that spillover of the adsorbate onto the catalyst support can result in the differences observed experimentally between desorption spectra obtained from single crystals and supported-metal catalysts. An isosteric Arrhenius analysis of the TPD spectra has been used to demonstrate that, at low surface coverage, the activation energy characterising surface diffusion of adsorbates on the catalyst support can be obtained from the desorption spectrum.

**Keywords:** temperature-programmed desorption, spillover, supported-metal catalysts

## 1. Introduction

Temperature-programmed desorption (TPD) spectroscopy is a powerful technique for probing the structure of metallic catalysts *in situ*. The application of this method to the study of supported-metal catalysts, as opposed to single crystals, has, however, been limited by the difficulty in interpreting the complex desorption spectra obtained from oxide-supported metals. The differences in the desorption spectra of supported and unsupported metallic catalysts are frequently attributed to the spillover of the adsorbate onto the catalyst support [1]. This is illustrated by the desorption of hydrogen from unsupported Pt [2], highly dispersed Pt/silica catalysts [3], and microfabricated Pt/silica catalysts [4]. In the case of Pt/silica the desorption peaks obtained from the supported catalysts are found to be broader than those obtained from the unsupported metal, and additional desorption peaks, attributed to irreversibly adsorbed hydrogen, are observed. Similar spectral features are obtained for Pt and Pt/alumina catalysts [1,5].

Monte Carlo simulations of desorption from single-crystal surfaces have been conducted previously by a number of authors and illustrate the limitations of the approximate mean-field or lattice gas approximations frequently used for the interpretation of TPD spectra [6–8]. In this paper, we extend previous simulations to consider desorption from surfaces representative of oxide-supported metallic catalysts. A Monte Carlo model for the second-order desorption from the surface of a supported-metal catalyst is introduced and an isosteric analysis conducted to determine the apparent Arrhenius parameters for the desorption process. It is demonstrated that both multiple desorption peaks and peak broadening can be attributed to adsorbate spillover and surface diffusion. It is further shown that the

size and geometry of the metal crystallites do not influence the desorption spectra to a significant extent.

## 2. Model and algorithm

The surface of the supported-metal catalyst is represented by a simulation lattice consisting of a regular square array of discrete surface sites. Each site is taken to represent either a region of the catalyst support or an adsorption site on a metal crystallite. The regions of the catalyst surface occupied by the metal crystallites and those representing the catalyst support are determined by constructing a Voronoi tessellation of the plane [9]. The tessellation algorithm divides the surface into a number of irregular polygons, each of which is randomly assigned as either a region of catalyst support or as a metal particle. The simulation lattice represents a projection of the actual catalyst surface onto the plane, producing an image of the surface similar to that obtained from electron micrographs of supported-metal catalysts. Examples of simulation lattices with increasing metal loadings are shown in figure 1. Increasing the number fraction,  $\phi$ , of the regions representing the metallic crystallites leads to the coalescence of these regions, with a resultant increase in the mean metal particle size.

As hydrogen chemisorption and temperature-programmed reduction are the most important experimental applications of TPD spectroscopy, this paper will consider the simulation of hydrogen desorption from a supported transition metal catalyst. The desorption process is therefore assumed to be second order.

It is assumed that hydrogen adsorbs from the gas phase on the metal crystallites only. On adsorption the hydrogen atom is assumed to dissociate immediately, occupying a pair of neighbouring lattice sites. Although adsorption

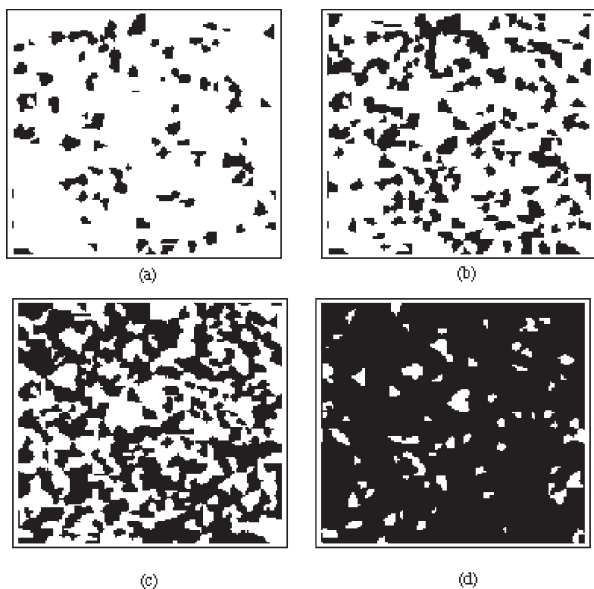


Figure 1. Example simulation lattices of supported-metal catalysts characterised by increasing metal loading and particle size. Panels represent fractional metal coverages of (a) 0.10, (b) 0.25, (c) 0.50, and (d) 0.75. The white and black regions represent the catalyst support and metal surface, respectively.

is only permitted on the metallic crystallites, and not on the catalyst support, the dissociated atoms can migrate by surface diffusion from the metal particles onto the catalyst support. Similarly, the recombination and subsequent desorption of hydrogen is only permitted on the metal crystallites. Desorption from the metal crystallites and surface diffusion, both on the oxide support and the metal crystallites, are assumed to be activated processes, the rate of each process being characterised by the appropriate Arrhenius expression.

The activation energy of desorption,  $E_a$ , is determined by the intrinsic activation energy associated with the adsorption site and the lateral interaction energy between neighboring adsorbate molecules, where

$$E_a = E_a^0 + n_p \varepsilon. \quad (1)$$

In equation (1)  $n_p$  is the number of adsorbate molecules neighbouring a pair of dissociated atoms and  $\varepsilon$  is the lateral interaction energy between nearest-neighbour adsorbate pairs. For a pair of dissociated atoms on the surface of a square lattice  $0 \leq n_p \leq 6$ . The activation energy for the recombination and desorption of a pair of isolated dissociated atoms as molecular hydrogen is denoted by  $E_a^0$ .

Previous Monte Carlo studies of thermal desorption either neglect surface diffusion entirely [10] or, as it is usually the case that the activation energy characteristic of surface diffusion is lower than that for desorption, the adlayer is allowed to reach thermal equilibrium between subsequent desorption events [11]. The latter situation is a reasonable assumption for the diffusion of dissociated hydrogen atoms on metal surfaces, but not for the diffusion of spillover hydrogen on an oxide support.

The mechanism of surface diffusion is quite different on the metal crystallites and on the catalyst support. The activation energy for surface diffusion on the metal crystallites is often low, typically of the order of  $10 \text{ kJ mol}^{-1}$ . Thus, the rate of surface diffusion on the metallic crystallites is likely to be rapid compared to either the rate of diffusion on the metal-oxide support or the rate of desorption. For this reason diffusion on the metal crystallites was simulated by allowing the atoms adsorbed on the metal crystallites to diffuse until thermal equilibrium had been attained.

Dissociated atoms adsorbed on the metallic crystallites are assumed to diffuse across the surface by a series of uncorrelated jumps between neighbouring lattice sites. The activation energy for the diffusion of a dissociated atom on a metallic crystallite,  $E_m$ , from site  $(i, j)$  to a neighbouring site  $(i', j')$  can be approximated by the intersection between two adjacent harmonic potentials and the energy minimum to give

$$E_m = E_m^0 - \delta E/2 + \frac{\delta E^2}{16E_m^0}. \quad (2)$$

In equation (2) the activation barrier for the diffusion of an isolated atom is given by  $E_m^0$  and the energy difference,  $\delta E$ , between an atom located at  $(i, j)$  and  $(i', j')$  by

$$\delta E = \varepsilon(n_{ij} - n_{i'j'} - 1), \quad (3)$$

where  $n_{ij}$  denotes the number of adsorbate atoms neighbouring site  $(i, j)$ .

Metropolis minimisation has been used to relax the adatoms on the metal crystallites. An adsorbate atom located on a metal adsorption site  $(i, j)$  is selected at random and an attempt made to diffuse the atom to a neighboring adsorption site  $(i', j')$  on the metal surface. If a vacant neighboring site is found, one site is selected at random and the particle moved to the new site with a probability,  $P_t$ , given by

$$P_t = \min[\exp(-E_m/RT), 1]. \quad (4)$$

This process is repeated until thermal equilibrium is attained.

The mechanism for the diffusion of spillover hydrogen on the oxide support is assumed to be the exchange of the terminal hydrogens of neighbouring hydroxyl groups, a process with a significantly higher characteristic activation energy than that of the diffusion of hydrogen on the metal crystallites. It is therefore assumed that the diffusion of hydrogen on the oxide support can be described by a random walk on the support regions of the surface. Isotope exchange experiments suggest that the activation energy for the exchange of spillover hydrogen with the surface silanol groups of silica,  $E_s$ , is approximately  $30 \text{ kJ mol}^{-1}$ ; the corresponding value for diffusion on alumina is over  $75 \text{ kJ mol}^{-1}$  [12]. Lateral interactions between adjacent hydroxyl groups are neglected.

As the time scales characteristic of surface diffusion on the metal crystallites and desorption can differ by several orders of magnitude, the explicit inclusion of diffusion in

addition to desorption requires the use of a highly efficient Monte Carlo algorithm. To allow for the simulation of events occurring over widely differing time scales an algorithm based on the method of logarithmic classes [13] has been developed, and is implemented as follows:

- (1) The catalyst surface is populated with adsorbate atoms until all the metal adsorption sites are occupied. The simulated reduction of the catalyst is carried out at high temperature, allowing the dissociated adsorbate atoms to diffuse freely across the catalyst support where appropriate.
- (2) Each possible desorption or hydrogen exchange event is then assigned to one of a number of event lists, with each list being comprised of all events with similar rates. The rate of each possible desorption or diffusion event,  $r_e$ , is calculated and assigned to a list,  $l_n$ , such that

$$n = \text{Floor}\{\log_2(r_e)\}. \quad (5)$$

The rates of any two members of a given list do not therefore differ by more than a factor of 2. The bounds on the rates of the events in a given class are thus given by

$$2^n < r_e < 2^{n+1}. \quad (6)$$

Both the rate of hydrogen desorption and hydrogen diffusion on the oxide support are assumed to be activated processes. The rate of each event,  $r_e$ , will therefore be determined by the Arrhenius expression describing either the rate of desorption,  $r_d$ , or the rate of surface diffusion on the support,  $r_s$ . Only diffusion on the oxide support and desorption is considered at this stage, diffusion on the metal crystallites is considered in step 4.

- (3) The probability of selecting a particular list is proportional to the rate associated with a given list and the number of events on the list. Once a list is selected, an event is then selected from the list at random and the lattice updated. The distribution of waiting times between subsequent events,  $\delta t$ , is given by a Poisson distribution [14], therefore

$$\delta t = -\frac{\ln \rho}{\sum r_e}, \quad (7)$$

where  $\rho$  is a uniformly distributed random number between 0 and 1.

- (4) The adsorbates on the metal crystallite regions of the surface are allowed to diffuse until an equilibrium adsorbate configuration is achieved.
- (5) Finally, the temperature is increased by an increment  $\delta T = \beta \delta t$ , where  $\beta$  is the heating rate.

In all simulations the activation energy and pre-exponential factor for the desorption process were taken to be

$100 \text{ kJ mol}^{-1}$  and  $1 \times 10^{13} \text{ s}^{-1}$ , respectively. These values are typical for the desorption of hydrogen from transition metal surfaces [15]. A lateral interaction energy of  $\pm 2 \text{ kJ mol}^{-1}$  was used. The mechanism of hydrogen diffusion on the support surface was assumed to be the exchange of hydrogen between adjacent silanol groups, and an activation energy of  $30 \text{ kJ mol}^{-1}$  was assumed unless otherwise stated. This assumption was based on the results of isotope exchange [12] and infrared studies [16] of surface diffusion on silica. The pre-exponential factor for surface diffusion was estimated to be  $1 \times 10^6 \text{ s}^{-1}$  [15].

All Monte Carlo simulations were conducted on lattices composed of  $256^2$  adsorption sites and the desorption spectra obtained from an average of 100 simulations. Simulations were implemented in C++ using software developed by the authors [17].

### 3. Results and discussion

We first consider the case where adsorbate spillover is assumed not to occur and the dissociated hydrogen atoms are confined to the individual metal crystallites. These simulations enable the extent to which metal particle geometry and size influence the simulated TPD spectrum to be determined. Desorption spectra for a number of simulation lattices for non-interacting adsorbates and for attractive lateral interactions are presented in figure 2. In the absence of lateral interactions, the desorption spectrum obtained is found to independent of  $\phi$ , the metal loading, and thus of the metal crystallite size. This result is to be expected as all the possible adsorbate configurations on a given crystallite are energetically equivalent for  $\varepsilon = 0$ . For the case of attractive lateral interactions, the desorption peak is found to become wider and the desorption rate maximum is displaced to a lower temperature as the particle size decreases. This is due both to the constrained diffu-

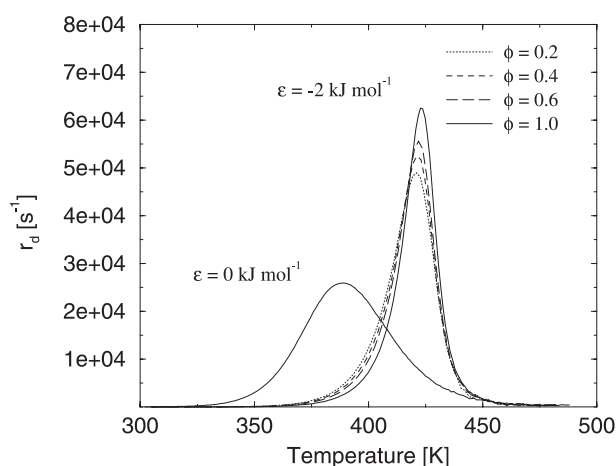


Figure 2. Predicted spectra of hydrogen desorption from simulated supported-metal catalysts with metal loading as a parameter. The rate of desorption,  $r_d$ , as a function of temperature is shown for non-interacting adsorbates ( $\varepsilon = 0 \text{ kJ mol}^{-1}$ ) and attractive lateral interactions ( $\varepsilon = -2 \text{ kJ mol}^{-1}$ ). Data are shown for a heating rate of  $20 \text{ K s}^{-1}$ .

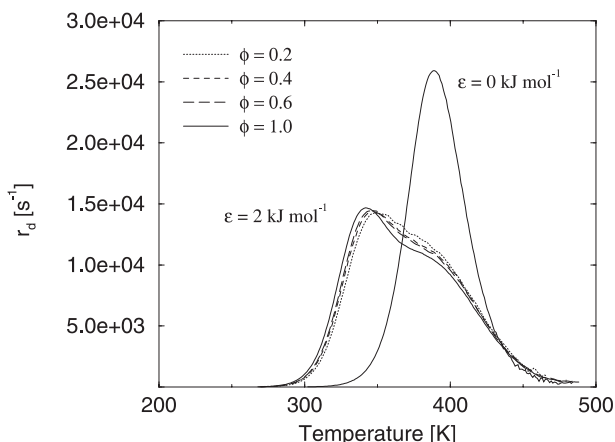


Figure 3. Predicted spectra of hydrogen desorption from simulated supported-metal catalysts for non-interacting adsorbates ( $\epsilon = 0 \text{ kJ mol}^{-1}$ ) and repulsive lateral interactions ( $\epsilon = 2 \text{ kJ mol}^{-1}$ ). Data are shown for a heating rate of  $20 \text{ K s}^{-1}$ .

sion of the adsorbate atoms on the more tortuous surface of the smaller particles and to the influence of the low coordination sites at the particle boundaries. It is, however, more likely that adsorbate–adsorbate interactions will be repulsive rather than attractive, and the corresponding spectra for repulsive interactions are given in figure 3. In the case of repulsive lateral interactions, the displacement of the desorption rate maximum is of a similar magnitude to that for attractive lateral interactions. The desorption peak is found to be displaced to higher temperature and broaden slightly as the metal particle size declines.

The dependence of the desorption activation energy on surface coverage can be quantified by conducting an isosteric analysis of the desorption spectrum [18]. In general, the distribution of adsorbates on the catalyst surface will be non-random and the Polanyi–Winger equation for the rate of desorption,  $r_d$ , becomes

$$r_d = \nu_0 \exp(-E_a/RT) \Phi(\theta), \quad (8)$$

where  $\Phi(\theta)$  is an unknown function representing the probability of a pair of neighboring lattice sites being occupied. Equation (8) reduces to the more familiar form where  $\Phi(\theta) = \theta^2$  only as  $T \rightarrow \infty$ . By conducting a number of simulations at various heating rates the Arrhenius parameters for desorption at constant coverage can be obtained using the isosteric method of Taylor and Weinberg [18]. Using this analysis, the activation energy is given by

$$E_a(\theta) = - \left[ \frac{\partial \ln r_d}{\partial (1/RT)} \right]_{\theta}. \quad (9)$$

This result is independent of the unknown function  $\Phi(\theta)$  allowing for the activation energy to be determined even if  $\Phi(\theta) \neq \theta^2$ . The pre-exponential factor cannot, however, be determined as

$$\nu_0 = \lim_{T \rightarrow \infty} \frac{r_d}{\Phi(\theta)}. \quad (10)$$

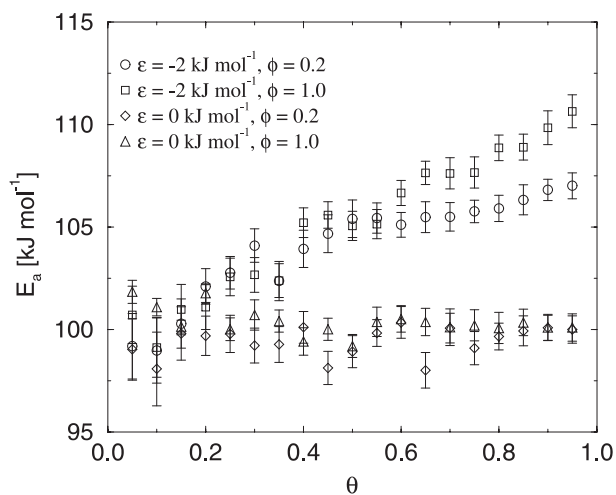


Figure 4. The results of an isosteric Arrhenius analysis of the desorption spectra for a highly dispersed supported-metal catalyst ( $\phi = 0.2$ ) and the corresponding single-crystal surface ( $\phi = 1.0$ ). Data are shown for attractive ( $\epsilon = -2 \text{ kJ mol}^{-1}$ ) and no lateral interactions. Error bars indicate the 95% confidence interval.

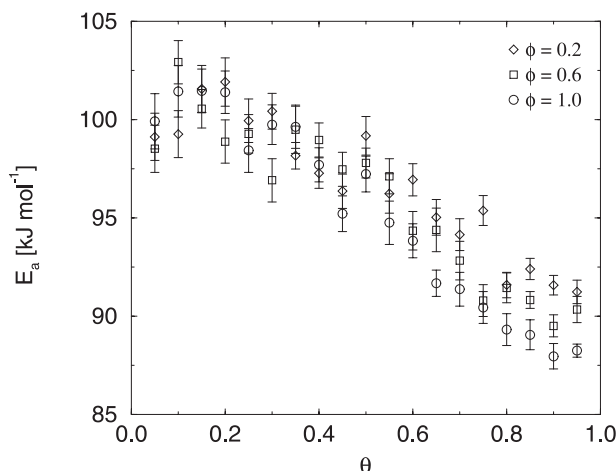


Figure 5. The results of an isosteric Arrhenius analysis of the desorption spectra for a highly dispersed supported-metal catalyst and single-crystal surface for repulsive lateral interactions ( $\epsilon = 2 \text{ kJ mol}^{-1}$ ). Error bars indicate the 95% confidence interval.

Results for the desorption of adsorbates with attractive lateral interactions are compared to those in the absence of lateral interactions in figure 4. The corresponding results for repulsive interactions are given in figure 5. For the case of attractive interactions the activation energy of desorption for  $\phi = 1.0$  declines from  $E_a \approx E_a^0 + 6\epsilon$  at monolayer coverage to  $E_a^0$  at  $\theta = 0$ . The influence of a finite particle size is only noticeable at high surface coverage where the preferential desorption of adsorbates at the particle edges leads to the result that  $E_a \leq E_a^0 + 6\epsilon$  for  $\theta = 1$ . The corresponding analysis for a single-crystal surface with no lateral interactions is shown for comparison. For repulsive lateral interactions an analysis of three surfaces characterised by different metal loadings leads to a very similar dependence of the desorption activation energy on the surface coverage for each surface. We now consider the case of adsor-

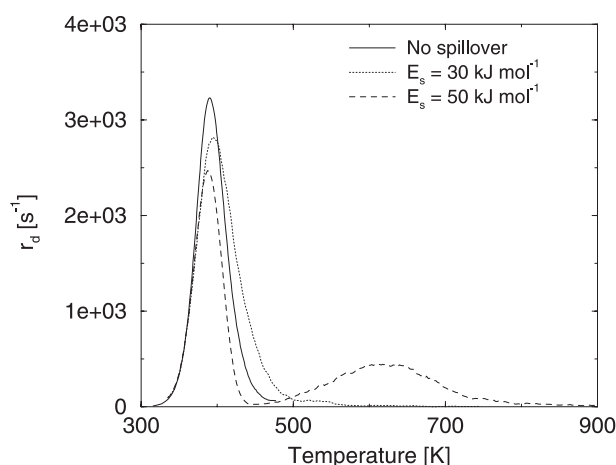


Figure 6. Predicted spectra of hydrogen desorption from a simulated supported-metal catalyst where adsorbate spillover onto the catalyst support occurs. Data are presented for two values of the diffusion activation energy illustrating both peak broadening and peak splitting. Spectra are shown for  $\varepsilon = 0$ . Data are shown for a heating rate of  $20 \text{ K s}^{-1}$ .

bate spillover, where the dissociated adsorbate molecules are free to diffuse across the catalyst support. The activation energy of surface diffusion on the catalyst support may be obtained if it is assumed that the rate of diffusion on the catalyst support,  $r_s$ , is also governed by an Arrhenius equation, where

$$r_s = \nu'_0 \exp(-E_s/RT) \Phi'(\theta). \quad (11)$$

In equation (11)  $\nu'_0$  and  $E_s$  represent the pre-exponential factor and activation energy for surface diffusion respectively. The probability of a vacant site neighbouring an occupied site is denoted by  $\Phi'(\theta)$ .

In figure 6 the simulated TPD spectra are shown for two values of activation energy of surface diffusion. At high adsorbate surface coverage the rate-limiting step for desorption is the recombination of the dissociated molecule on the metal particles and the characteristic activation energy of desorption for  $\theta \approx 1$  is  $E_a$ . At low surface coverage, however, the rate-limiting step is the diffusion of the spillover hydrogen across the support surface back to the metallic particles where desorption can occur. Thus, the rate-limiting step for desorption will be the diffusion of any spillover adsorbate back to the metal particles and the apparent activation energy for desorption will be equal to  $E_s$  as  $\theta \rightarrow 0$ .

If the activation energy of surface diffusion is sufficiently high, corresponding to the spectrum generated using  $E_s = 50 \text{ kJ mol}^{-1}$ , then the transition between diffusion-limited and recombination-limited desorption will be discontinuous. The discontinuous transition corresponds to the removal of all the adsorbate from the metal crystallites. At this point the spillover hydrogen is not sufficiently mobile to diffuse across the surface to the metallic crystallites and desorb. If the activation energy of diffusion is somewhat lower, as shown for the spectrum generated using  $E_s = 30 \text{ kJ mol}^{-1}$ , then the transition

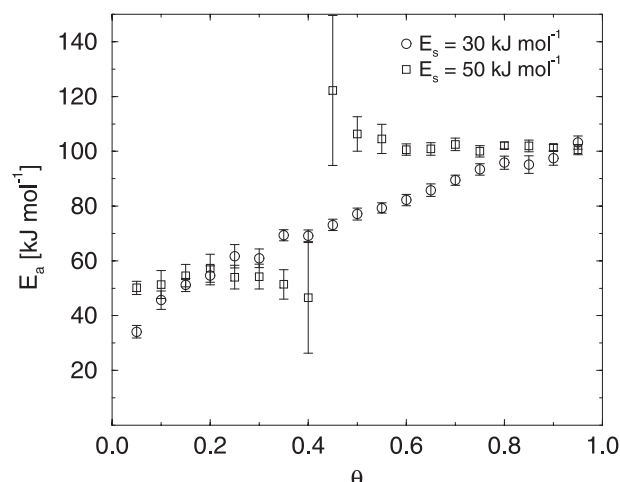


Figure 7. The results of the isosteric Arrhenius analysis of the spectra presented in figure 6. A discontinuity occurs where peak splitting is observed in the corresponding desorption spectra. Error bars indicate the 95% confidence interval.

from the desorption rate being limited by recombination to diffusion-limited behavior is continuous. The results of an isosteric analysis of these spectra are presented in figure 7.

The influence of hydrogen spillover on the apparent activation energy of desorption could be misinterpreted as representing a wide distribution of the true activation energy of desorption. Data of this nature have been reported in the literature for desorption from supported-metal catalysts. In a study of hydrogen desorption from Ni/silica [19] an approximately uniform activation energy distribution between  $30 \text{ kJ mol}^{-1}$  at  $\theta = 0$  and  $110 \text{ kJ mol}^{-1}$  at  $\theta = 1$  was obtained. This result corresponds to a linear variation of activation energy with surface coverage similar to that shown in figure 7. Similar data have also been reported for Pt/silica catalysts [20]. It is implied from the current study that such data do not represent a distribution of desorption activation energies from a heterogeneous surface but are, instead, indicative of a surface diffusion-limited process.

#### 4. Conclusions

We have extended previous Monte Carlo simulations of desorption from unsupported metals to consider the second-order desorption of hydrogen from oxide-supported metallic catalysts. A geometric representation of a supported-metal catalyst, based on a Voronoi tessellation of the plane, has been used to represent catalysts with various metal particle-size distributions. The extent to which surface geometry and adsorbate spillover determine the features of the desorption spectra has been studied. By conducting an isosteric Arrhenius analysis of the TPD spectrum obtained from these surfaces it has been shown that the influence of metal particle size on the desorption spectra is unlikely to be significant. This result supports previ-

ous numerical studies [9] suggesting that nano-fabricated model catalysts, consisting of regular metal arrays on an oxide support, provide model catalyst systems that are representative of the more complex surfaces of dispersed metal catalysts.

The inclusion of adsorbate spillover and surface diffusion is found to result in a broadening, and eventual splitting, of the desorption peak compared to the results obtained for the corresponding single crystal. These predictions are in agreement with experimental results for supported and un-supported metal catalysts. The possibility of misinterpreting a diffusion-limited desorption process as representing a distribution of desorption activation energy from a heterogeneous surface has been demonstrated. It is further shown that the activation energy for surface diffusion may be obtained in the low surface coverage limit from an isosteric analysis of the desorption spectrum.

### Acknowledgement

ASM thanks Peterhouse, Cambridge, for the award of the Rolls-Royce Frank Whittle Research Fellowship.

### References

- [1] P. Ferreira-Aparicio, A. Guerrero-Ruiz and I. Rodriguez-Ramos, *J. Chem. Soc. Faraday Trans.* 93 (1997) 3563.
- [2] S. Tsuchiya, Y. Amenomiya and R.J. Cvetanovic, *J. Catal.* 19 (1970) 245.
- [3] J.T. Miller, B.L. Meyers, F.S. Modica, G.S. Lane, M. Vaarkamp and D. Koningsberger, *J. Catal.* 143 (1993) 395.
- [4] P.W. Jacobs, S.J. Wind, F.H. Ribeiro and G.A. Somorjai, *Surf. Sci.* 372 (1997) L249.
- [5] H. Ehwald and U. Leibnitz, *Catal. Lett.* 38 (1996) 149.
- [6] J.L. Sales and V.P. Zhdanov, *Surf. Sci.* 209 (1989) 208.
- [7] S.J. Lombardo and A.T. Bell, *Surf. Sci.* 206 (1988) 101.
- [8] B. Meng and W.H. Weinberg, *J. Chem. Phys.* 100 (1994) 5280.
- [9] A.S. McLeod and L.F. Gladden, *J. Catal.* 173 (1998) 43.
- [10] M. Meng, P.Y. Lin and Y.L. Fu, *Catal. Lett.* 48 (1997) 213.
- [11] B. Meng and W.H. Weinberg, *J. Chem. Phys.* 102 (1995) 1003.
- [12] D. Martin and D. Duprez, *J. Phys. Chem.* 101 (1997) 4428.
- [13] T. Fricke and D. Wendt, *Int. J. Mod. Phys. C* 6 (1997) 277.
- [14] D. Gillespie, *J. Comput. Phys.* 22 (1976) 403.
- [15] V.P. Zhdanov, *Surf. Sci. Rep.* 12 (1991) 183.
- [16] R. Kramer and M. Andre, *J. Catal.* 58 (1979) 287.
- [17] A.S. McLeod, Ph.D. thesis, University of Cambridge (1997).
- [18] J.L. Taylor and W.H. Weinberg, *Surf. Sci.* 78 (1978) 259.
- [19] M. Arai, M. Fukushima and Y. Nishiyama, *Appl. Surf. Sci.* 99 (1996) 145.
- [20] M. Arai, Y. Nishiyama, T. Masuda and K. Hashimoto, *Appl. Surf. Sci.* 89 (1996) 11.